# Fabrication of Dense $ZrO_2$-$Al_2O_3$ Composite Ceramics by Pulsed Electric-Current Pressure Sintering of Neutralization Co-Precipitated Powders

Ken HIROTA*, Kenta YAMAMOTO*, Koki SASAI*, Masaki KATO*, Hideki TAGUCHI**
Hideo KIMURA***, Masayuki TAKAI***, Masao TERADA***

(Received February 27, 2017)

$ZrO_2$-based composite ceramics containing 25 mol% $Al_2O_3$ and 1.125 mol% $Y_2O_3$, *i.e.*, with a composition of 75mol%$ZrO_2$(1.5mol%$Y_2O_3$)-25mol%$Al_2O_3$, were fabricated using pulsed electric-current pressure sintering (PECPS) of solid solution powders prepared by the neutralization co-precipitation method. They were sintered at 1573 to 1623 K (1300~1350°C) for $6.0\times10^2$ s (10 min) under 50 MPa in Ar. Thus-obtained ceramics consisted of 130~150 nm grains, composed of α-$Al_2O_3$ and tetragonal-$ZrO_2$ with a small amount of monoclinic-$ZrO_2$. Dense ceramics with high relative densities ≥99.5% revealed high mechanical properties: bending strength ($\sigma_b$) higher than 1.3 GPa and simultaneous fracture toughness ($K_{IC}$) higher than 15.5 MPa·$m^{1/2}$, which value was evaluated by the indentation fracture toughness (IF) test. X-ray diffraction (XRD) analysis, scanning electron microscope (SEM) and transmission electron microscope (TEM) with energy dispersive X-ray spectrometry (EDS) observations on the as-prepared and calcined powders, and the microstructures of ceramics demonstrated the homogeneous grain distribution of *t*-$ZrO_2$ and α-$Al_2O_3$, with the former grains being surrounded by the latter which had segregated from the calcined cubic $ZrO_2$ solid solution containing both $Al_2O_3$ and $Y_2O_3$.

**Key words :** zirconia, alumina, mechanical properties, co-precipitation, pulsed electric-current pressure sintering

## 1. Introduction

Following the discovery of the stress-induced transformation $ZrO_2$-toughening mechanism from tetragonal to monoclinic phases by Garvie [1], partially stabilized zirconia (PSZ) with a small amount of $Y_2O_3$ addition has been a major research focus, and many studies have been performed on the fabrication of dense PSZs with other added stabilizer [2-6].

Table 1. Mechanical properties of representative partially stabilized zirconia.

| | Content of additives (mol%) | Vickers hardness *Hv* (GPa) | Young's modulus *E* (GPa) | Bending strength $\sigma_b$ (MPa) | Fracture toughness $K_{IC}$ (MPa・$m^{1/2}$) |
|---|---|---|---|---|---|
| Y-PSZ *($Y_2O_3$) | 2.2 | 13.6 | 233 | 1384 | 6.9 |
| Ca-PSZ* (CaO) | 16 | 17.2 | 210 | 241 | 2.5 |
| Mg-PSZ* (MgO) | 6.9 | 14.4 | 200 | 685 | 4.8 |
| Al-PSZ ($Al_2O_3$) | 25 | — | — | 570$^{\$}$ | 23$^{\&}$ |

*: Partially stabilized zirconia.
$: determined using an 8mm-length span.
&:determined by the indentation fracture (IF) method [13] with Niihara's equation [14].

* Department of Molecular Chemistry and Biochemistry, Faculty of Science and Engineering, Doshisha University, Kyoto 610-0321, Japan, Telephone: +81-774-65-6690, Fax: +81-774-65-6849, E-mail: khirota@mail.doshisha.ac.jp
**The Graduate School of Natural Science and Technology (Science), Okayama University, Okayama 700-8530, Japan
***Daiichi Kigenso Kagaku Kogyo Co., Ltd., Hirabayashi-minami Suminoe-ku, Osaka 559-0025, Japan

Table 1 shows the mechanical properties of the representative PSZs, some of which are commercially available now. In addition, $ZrO_2(Y_2O_3)$-based and $ZrO_2(Y_2O_3)$-$Al_2O_3$ composite ceramics fabricated using hot pressing (HP) and hot isostatic pressing (HIP) have been developed [7-10].

On the other hand, little attention has been paid to the solid solution (*ss*) in the $ZrO_2$-$Al_2O_3$ system, because it had been believed that the $ZrO_2$-$Al_2O_3$ system did not form the (*ss*) even at high temperatures. However, since the report by Alper [11] on the formation of $ZrO_2$(*ss*) containing 7 mol% $Al_2O_3$, sol-gel derived $ZrO_2$(*ss*) powders have been prepared and 75mol%$ZrO_2$ -25mol%$Al_2O_3$(*ss*) powders were hot isostatic press (HIP) sintered at 1373 K (1100°C) under 196 MPa for $3.6\times10^4$ s (1 h) [12]. Evaluation of their mechanical properties revealed a fracture toughness ($K_{IC}$) of 23 MPa·$m^{1/2}$ which was estimated by the indentation fracture toughness (IF) method [13] with a Niihara's equation [14], (afterwards, the value of $K_{IC}$ estimated using this IF method is described in the present study without any comment), however, the bending strength ($\sigma_b$) remained as low as 570 MPa. Since this investigation, there has been no report on the fabrication of dense monolithic or composite ceramics that showed a high strength $\sigma_b \geq 1$ GPa and a high fracture toughness $K_{IC} \geq 20$ MPa·$m^{1/2}$ at the same time. If bulk ceramics with both a high strength and high fracture toughness simultaneously could be developed, this would do away with the concept of ceramics as "brittle" and promote their application in a wide range of fields.

In 2012, it was shown that 75mol% $ZrO_2$(1.2~1.5mol%$Y_2O_3$)-25mol%$Al_2O_3$ composite ceramics fabricated using pulsed-electric current pressure sintering (PECPS) [15,16] of the sol-gel derived cubic $ZrO_2$(*ss*) powders containing both $Al_2O_3$ and $Y_2O_3$ revealed high $K_{IC} \geq 20.0$ MPa·$m^{1/2}$, and at the same time, high $\sigma_b \geq 1.0$ GPa [17,18].

On the other hand, as the sol-gel powder preparation is very expensive due to the high costs of the starting materials and its complex process, this method is not suitable for the mass-production requirements of the ceramics industry. Therefore, there is much requirement of a low-cost method for producing homogeneous fine-particle powders.

Accordingly, the neutralization co-precipitation method [19], using an aqueous solution, has been considered as a low-cost process for the preparation of (*ss*) powders corresponding to $ZrO_2(Y_2O_3)$-$Al_2O_3$. Here, we should note that the sol-gel method can produce fine powders with the homogeneous chemical composition and particle shape, and sharp particle size distribution[20].

In the present study, the following subjects are considered: (1) the optimum content of stabilizer $Y_2O_3$ for $ZrO_2$ to attain a high tetragonal $ZrO_2$ (*t*-$ZrO_2$) ratio in order to utilize the transformation toughening mechanism, (2) the improvement of both the chemical homogeneity of intra-particles and the particle size distribution, and (3) the optimum process conditions, especially the sintering temperature, and (4) by following the guiding principle for fabricating high-strength $ZrO_2$ ceramics to achieve a small grain size ≤1.0 μm, a high relative density ≥99.5% and high *t*-$ZrO_2$ ratios. As a result, we fabricated $ZrO_2(Y_2O_3)$-$Al_2O_3$ composite ceramics exhibiting high $\sigma_b$ and $K_{IC}$ simultaneously from the neutralization co-precipitated powder for the first time. This paper deals with their mechanical properties in relation with the microstructures depending on the $Y_2O_3$ content and chemical homogeneity of intra-particles calcined powders.

## 2. Experimental Procedure

### 2.1 *Fabrication of $ZrO_2$ ($Y_2O_3$) - $Al_2O_3$ ceramics*

Solid solution powders with compositions of 75mol%$ZrO_2$(*x*·mol%$Y_2O_3$)–25mol%$Al_2O_3$ (*x*=0.5, 1.0, 1.5, 2.0), *i.e.*, $ZrO_2$ : $Y_2O_3$ : $Al_2O_3$ = 74.625 ~ 73.50 : 0.375 ~ 1.50 : 25.0 mol% [17,18], were prepared by the neutralization co-precipitation method [19] using high quality reagents (≥99.9% pure) of $ZrOCl_2 \cdot 8H_2O$, $YCl_3$,

and $AlCl_3$ as the starting materials and aqueous $NH_3$ solution as a pH adjuster, all of these are commercially available. The TEM photograph and X-ray diffraction (XRD) pattern of the as-prepared powders (precursor) shown in Fig. 1(a) and (b), respectively, revealed that they are fine amorphous powders.

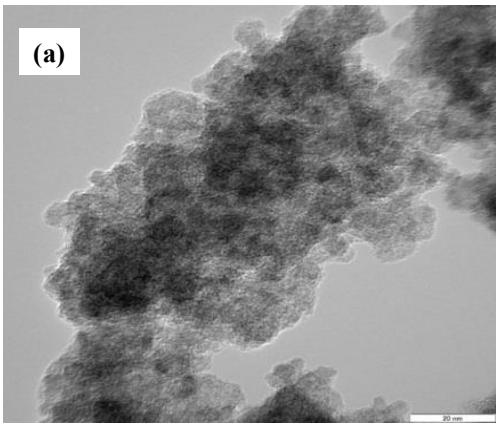


$<P_s>$: 0.5 nm

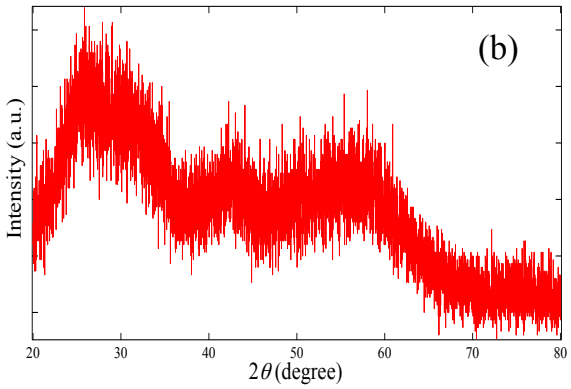


Fig. 1. (a) TEM photograph and (b) XRD pattern of $ZrO_2$(1.5mol%$Y_2O_3$)-25mol%$Al_2O_3$ powder as-prepared by the neutralization co-precipitation method.

Then, they were heat-treated (calcined) in two ways, as will be mentioned in a later section: by i) simple one-step calcination at 1173 K (900°C) for $3.6\times10^3$ s (1 h) or ii) a more complex two-step calcination, *i.e.*, the combination of a long low-temperature heating at 973 K (700°C) for $3.24\times10^4$ s (9 h) and a short high-temperature heating at 1173 K (900°C) for $3.6\times10^3$ s (1 h) in air. Both calcined powders were milled using an alumina-mortar and pestle for $1.8\times10^3$ s (30 min) in ethanol. After drying at 353 K (80°C) for $4.32\times10^4$ s (12 h) in a reduced pressure, a small amount of diluted poly-vinyl-alcohol (PVA) solution (a concentration of 3~5%) was added to the milled powders. Then, they were compacted into circular disks with the outer diameter (OD) about 15 mm and the thickness about 5.0 mm ($15^{\phi}$-$5.0^{h}$ mm) under a uniaxial pressure of 70 MPa followed by cold isostatic pressing (CIP) at 245 MPa for $1.8\times10^2$ s (3 min). The powder compacts with a relative density ($D_{g\text{-}bulk}/D_{g\text{-}x}$) of about 46~47%, where $D_{g\text{-}bulk}$ is the green bulk density (2.4~2.5 $Mg\cdot m^{-3}$) of powder compact and $D_{g\text{-}x}$ its theoretical density (5.3603 $Mg\cdot m^{-3}$) [21] were sintered with a pulsed electric-current pressure sintering (PECPS) apparatus (*SPS-5104A*; SPS SYNTEX Inc., Tokyo, Japan) with a heating rate of 1.667 $K\cdot s^{-1}$ (100 $K\cdot min^{-1}$: on-off interval=12:2), at 1573 to 1623 K (1300~1350°C) for $6.0\times10^2$ s (10 min) under 50 MPa using a carbon mold ($^{\phi}$40-$^{\phi}$16-$30^{h}$ mm) and plungers ($^{\phi}$15.9-$40^{h}$ mm) in Ar.

### 2.2 *Evaluation of samples Microstructures*

A differential thermal and thermal gravimetry analyses (DT-TG 60H; Shimadzu, Kyoto, Japan) of the precursors were conducted in air with a heating rate of 0.1667 $K\cdot s^{-1}$ (10 $K\cdot min^{-1}$). Crystalline phases were identified by XRD analysis (Cu$K\alpha$ radiation, *Rint 2000*; Rigaku, Osaka, Japan). The volume fraction of the monoclinic $ZrO_2$ (*m*-$ZrO_2$) phase was determined from the peak intensity ratio of the sum of the monoclinic (111) and (11-1) diffraction peaks to the tetragonal (111) [22]. The bulk densities ($D_{obs}$) of sintered ceramics after polishing with a diamond paste (nominal size $^{\phi}$1~3 μm) were evaluated by the Archimedes method. In order to determine the theoretical densities ($D_x$) of ceramics the lattice parameters of the *t*-$ZrO_2$ and *m*-$ZrO_2$ phases were estimated using Rietveld analysis [23]. From the *t*/*m*-$ZrO_2$ volume ratios, the chemical composition, and the values of $D_x$(*t*-$ZrO_2$(*x*·mol%$Y_2O_3$)), $D_x$(*m*-$ZrO_2$ (*x*·mol%$Y_2O_3$)), and $D_x$(α-$Al_2O_3$)=3.987 (JCPDS: #10-0173) $Mg\cdot m^{-3}$, the $D_x$ values of sintered ceramics

were calculated. Hereafter, tetragonal $ZrO_2$ containing 0.5 mol% $Y_2O_3$, *i.e.*, *t*-$ZrO_2$(0.5mol%$Y_2O_3$), and 75 mol% $ZrO_2$(1.5mol%$Y_2O_3$)-25mol%$Al_2O_3$ are abbreviated as *t*-$ZrO_2$(0.5Y) and [1.5Y], respectively.

Microstructural observations on the as-prepared and calcined powders, and the fractured or polished surfaces of ceramics were conducted using a field emission-type transmission electron microscope (FE-TEM) (*JEM-2100F*; JEOL, Ltd., Tokyo, Japan) and a scanning electron microscope (FE-SEM) (*JSM-7001FD*; JEOL, Ltd.) equipped with an energy dispersive X-ray spectrometry (EDS) (*JED-2300/T* and *JED-2300/F*, respectively; JEOL, Ltd.). Before TEM observation, the specimens were processed to make them thinner using a focused ion beam (FIB) (*FB-2200*; Hitachi High-Tech Fielding Co., Ltd., Tokyo, Japan). The grain sizes were determined by an intercept method [24].

2.3 *Mechanical properties*

After the crystalline-phase identification, test bars (~3×3.5×11 $mm^3$) for mechanical- property measurements were cut from the as-sintered ceramics with a diamond cutting-blade, and then their four sides were polished to mirror surfaces with a diamond paste (nominal particle size $\phi$1~3 μm). Three-point bending strength ($\sigma_b$) was evaluated with a cross-head speed of $8.33\times10^{-3}$ mm·$s^{-1}$ (0.5 mm·$min^{-1}$) and an 8 mm-length span length using WC jigs. As this length was not so enough long to evaluate $\sigma_b$, however, because of the small samples about 13~14 mm in diameter, their best $\sigma_b$ values were re-measured using a long span as 30 mm for the validity check in accordance with Japanese Industrial Standard (JIS) R 1601. Vickers hardness ($H_v$) was measured using a Micro Vickers Hardness Tester (*HMV*; Shimadzu) with a duration time of 15 s and an applied load of 19.6 N. As to the measurement of $K_{IC}$, IF method with a Niihara's equation [14] ($K_{IC}$[Palmqvist crack [25]])=$0.012(E/H_v)^{2/5}\cdot(H_vP/L)^{1/2}$, here $E$ is Young's modulus, $P$ load and $l$ the average length from the indent corner to the edge of each crack, *i.e.*, Palmqvist crack length). In addition the relationship between $E$ and $H_V$ *i.e.*, $E$ *n*early equal to $20\cdot H_v$ [26] was adopted to draw a relative comparison in $K_{IC}$ values among the samples. From the optical microscopic observation their indents with a "$c/a$" ratio < 2.5 was confirmed, proving the availability of $K_{IC}$ [Palmqvist crack], here, $c$ is the radius of the surface crack, $a$ the half diagonal. Thus $K_{IC}$ was evaluated using a Vickers Hardness Tester (VMT-7; Matsuzawa Co., Ltd., Tokyo, Japan) with an applied load of 196 N and a duration time of 15 s. The $K_{IC}$ values will be discussed in the next "Results and discussion".

## 3. Results and Discussion

3.1 *Characterization of powders and microstructures of ceramics*

All DTA curves of the as-prepared powders showed an endothermic peak around 1093 K (820°C) irrespective of the $Y_2O_3$ content. From XRD analysis the crystalline phases of samples heated bellow and above this peak were amorphous and *c*-$ZrO_2$ phase, respectively, *i.e.*, this endothermic peak corresponds to the crystallization temperature ($T_x$). In order to improve both the chemical inhomogeneity of intra-particles and their particle size distribution, these powders were calcined at 973 K (700°C) for $3.24\times10^4$ s (9 h), since it was considered that a long heating at the temperature bellow $T_x$ would enhance the ionic movements or diffusion in each particle due to the amorphous state. In addition, it has been cleared from our previous experiments that crystallized powders yielded ceramics with higher density and mechanical properties than those from the amorphous powders.

Figure 2 shows the XRD patterns measured on the [0.5Y] ~ [2.0Y] powders after the calcination performed by the two-step heating; strong XRD peaks belong to *c*-$ZrO_2$ phase were observed and neither $Al_2O_3$ nor $Y_2O_3$ phases were detected, suggesting that *c*-$ZrO_2$(*ss*) containing both $Al_2O_3$ and $Y_2O_3$ were crystallized from

the amorphous powders. Then, the powder morphology was observed; TEM photographs of the [1.5Y] powders calcined under various conditions are shown in Fig. 3 (a)~(c); (a) calcined at 973 K for $3.24\times10^4$ s (700°C/9 h), (b) one-step, and (c) two-step calcinations. Their particle size ($P_s$) increased from around 6.5 (Fig. 3 (a)) to 9.5 (Fig. 3 (c)) nm with increasing heating temperature. Here, the effects of calcination conditions on the microstructure of ceramics were investigated.

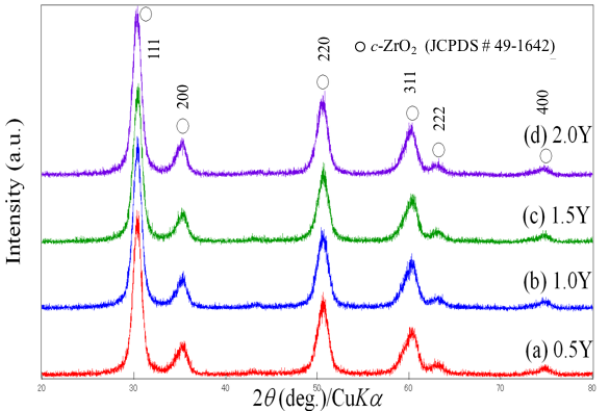


Fig. 2. XRD patterns of $ZrO_2$($x$·mol%$Y_2O_3$)-25mol%$Al_2O_3$ powders calcined at 973 K for $3.24\times10^4$ s (700°C/9 h) followed by heating at 1173 K for $3.6\times10^3$ s (900°C/1 h) in air.

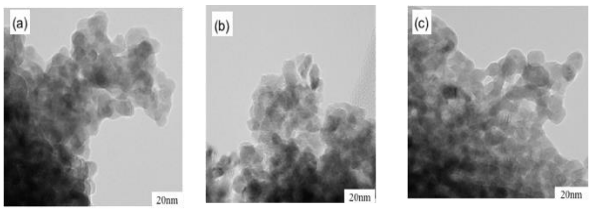


Fig. 3. TEM photographs of $ZrO_2$(1.5Y)-25mo%$Al_2O_3$ powders calcined at various conditions: (a) 973K/$3.24\times10^4$s (700°C/9 h), (b) 1173K/$3.6\times10^3$s (900°C/1 h) and (c) 973 K/$3.24\times10^4$s (700°C/9 h) + 1173 K/$3.6\times10^3$ s (900°C/1 h) in air.

Figure 4 shows SEM photographs of the polished surfaces for [1.5Y] ceramics fabricated at 1623 K using the calcined powders; from (a) one-step at 1173 K (900°C) for $3.6\times10^3$ s (1 h) and (b) two-step calcinations of 973 K (700°C) for $3.24\times10^4$ s (9 h) + 1173 K (900°C) for $3.6\times10^3$ s (1 h). In the left SEM photograph, large and coarse black particles of α-$Al_2O_3$ can be seen, while in the right photograph, fine and homogeneously dispersed α-$Al_2O_3$ are observed. Their mechanical properties were also evaluated; the left ceramics revealed a fracture toughness $K_{IC}$ of 9.39 MPa·$m^{1/2}$, while the right showed a $K_{IC}$ of 14.1~15.3 MPa·$m^{1/2}$ and a bending strength $\sigma_b$ of 1360~1390 MPa. By comparing these microstructure and mechanical properties, the two-step calcination was found to be suitable for the fabrication of $ZrO_2$($Y_2O_3$)-$Al_2O_3$ ceramics with high $K_{IC}$ and $\sigma_b$ than one-step heating. Therefore, we adopted the calcined powders under this combined heat treatment protocol in the subsequent experiments.

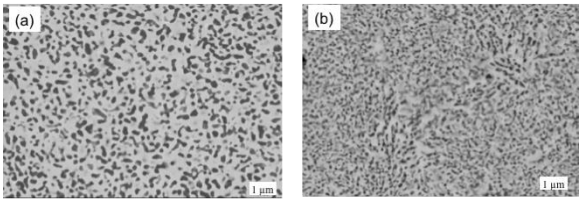


Fig. 4. SEM photographs of the polished surfaces for $ZrO_2$(1.5Y)-25mol%$Al_2O_3$ ceramics sintered at 1598~1623 K (1325~1350°C) using (a) a simple 1173 K for $3.6\times10^3$ s (900°C/1 h) and (b) a "two-step" 973 K for $3.24\times10^4$ s (700°C/9 h) and 1173 K for $3.6\times10^3$ s (900°C/1 h) calcined powders, respectively.

Figure 5 shows the XRD patterns of $ZrO_2$($x$·mol%$Y_2O_3$)-25mol%$Al_2O_3$ ceramics sintered at 1573K/$6.0\times10^3$s/60MPa (1300°C/10min/60MPa) with $x$ = (a) 0.5, (b) 1.0, (c) 1.5, and (d) 2.0, revealing clearly the presence of α-$Al_2O_3$ phase. In addition, by increasing the $Y_2O_3$ content, the monoclinic (JCPDS: #37-1484) *vs*. tetragonal $ZrO_2$ (JCPDS: #50-1089) ratio was much reduced. These results indicate that the $c$-$ZrO_2$($ss$) decomposed into α-$Al_2O_3$ and $ZrO_2$ with $Y_2O_3$ during PECPS, and that a small amount of $Y_2O_3$ could suppress the transformation from $t$-$ZrO_2$ to $m$-$ZrO_2$.

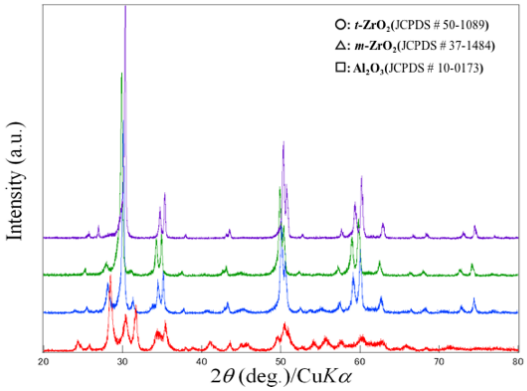


Fig. 5. XRD patterns of $ZrO_2$($x$·mol%$Y_2O_3$)-25mol%$Al_2O_3$ ceramics sintered at 1578K/ $6.0\times10^2$s/60MPa (1300°C/10min/60MPa); $x$= (a) 0.5, (b)1.0, (c) 1.5, and (d) 2.0.

Until now, there has been no report treating the theoretical density ($D_x$) of $t$-$ZrO_2$(0.5Y), $t$-$ZrO_2$(1.0Y), and $t$-$ZrO_2$(1.5Y), except for the study of lattice parameters of $t$-$ZrO_2$ and $c$-$ZrO_2$ phases which contained 2.0~6.6 mol% $Y_2O_3$ by Ingel *et al* [27]. They reported a measurement value of $D$($t$-$ZrO_2$(2.0Y)) =6.0880 Mg·m$^{-3}$ and a calculation value of $D$($t$-$ZrO_2$(2.0Y))=6.1067 Mg·m$^{-3}$ based on their lattice parameters.

From the lattice parameters of the $t$-$ZrO_2$ phase with the $Y_2O_3$ content 0.5 to 2.0 mol% estimated to be $a$=0.35999~0.36014 and $c$=0.52255~0.51814 nm, and those of $m$-$ZrO_2$ $a$=0.53232~0.51267, $b$=0.51927~0.51731, $c$=0.51591~0.53691 nm, and β= 98.87~98.92° by Rietveld analysis [23], the theoretical values of $D_x$($t$-$ZrO_2$(0.5Y))=6.0381, $D_x$($t$-$ZrO_2$(1.0Y))=6.0736, $D_x$($t$-$ZrO_2$(1.5Y))=6.0698, $D_x$($t$-$ZrO_2$(2.0Y))=6.0666 and $D_x$($m$-$ZrO_2$(0.5Y))=5.7580, $D_x$($m$- $ZrO_2$ (1.0Y))=5.7923, $D_x$($m$-$ZrO_2$(1.5Y))=5.7738 and $D_x$($m$-$ZrO_2$(2.0Y)) =5.7964 Mg·m$^{-3}$ were obtained. Comparing the present $D_x$($t$-$ZrO_2$(2.0Y)) =6.0666 with the values reported by Ingel *et al*. (6.0880~6.1067) Mg·m$^{-3}$, the former is slightly smaller; this could be explained in term of a small amount of oxygen deficiencies in the present ceramics induced during PECPS in a reduced oxygen pressure.

Using the $t$/$m$-$ZrO_2$ volume ratios, and the values of $D_x$($t$-$ZrO_2$($x$·mol%$Y_2O_3$)), $D_x$($m$-$ZrO_2$($x$·mol%$Y_2O_3$)), and $D_x$(α-$Al_2O_3$)=3.987 Mg·m$^{-3}$, the $D_x$ values of all of the ceramics sintered at 1598 K (1325°C) were calculated: $D_x$([0.5Y])=5.219, $D_x$([1.0Y])=5.238, $D_x$ ([1.5Y])=5.344, and $D_x$([2.0Y])=5.363 Mg·m$^{-3}$. Here, as the [0.5Y] ceramics sintered at 1598 K (1325°C) had many cracks and were broken during cutting and polishing, their $t$/$m$-$ZrO_2$ ratio was assumed to be about 5/95vol% from the pieces of broken ceramics, as will be shown in the following section. The bulk densities, except for the [0.5Y], were $D_{obs}$([1.0Y])=5.34, $D_{obs}$([1.5Y])=5.48 and $D_{obs}$([2.0Y])=5.41 Mg·m$^{-3}$. These values are a little higher than the theoretical values. This might be due to some errors originating from the Rietveld analysis and $t$-/$m$-$ZrO_2$ ratios determined with the method by Garvie and Nicholson [22].

Then, their microstructures were observed. Figure 6 shows FE-SEM photographs for the fracture surfaces of [1.5Y] ceramics sintered at: (a) 1573 K (1300°C), (b) 1598 K (1325°C) and (c) 1623 K (1350°C) for $6.0\times10^2$ s (10 min) under 50 MPa. The average grain sizes ($G_s$) determined using the intercept method [24] are also shown in these figures. From left to right, as the sintering temperature was raised, FE-SEM photographs taken as the secondary electron images demonstrate that the grains grew gradually from 130 to 150 nm in the dense homogeneous matrix. The effect of $Y_2O_3$ content on the microstructure was also investigated. Figure 7 shows SEM photographs for the fracture surfaces of the $ZrO_2$($x$·mol%$Y_2O_3$)-25 mol%$Al_2O_3$ ceramics sintered at 1598 K (1325°C) with $x$ = (a) 0.5, (b) 1.0, and (c) 2.0. These Figs. 6 and 7 display dense homogeneous microstructures with hardly any pores; proving the relative density ($D_{obs}$/$D_x$) must be more than 99.5%, as will be shown in Fig. 9. The values of $G_s$ indicate that the $Y_2O_3$ addition also suppresses the grain growth. For example, the $G_s$ of [0.5Y] ceramics was 440 nm, and then decreased to 220 [1.0Y], 140 nm [1.5Y] and 135 nm [2.0Y]. Thus, with increasing $Y_2O_3$ content, the $t$-$ZrO_2$ volume ratio increased and $G_s$ reduced.

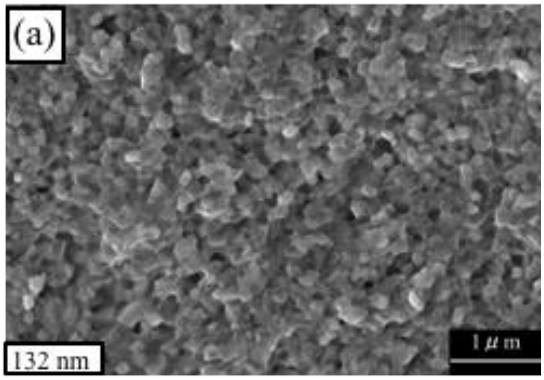


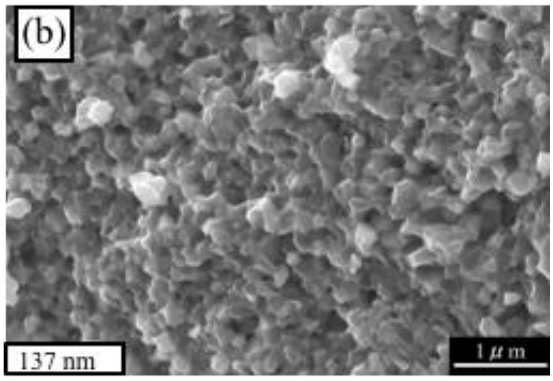


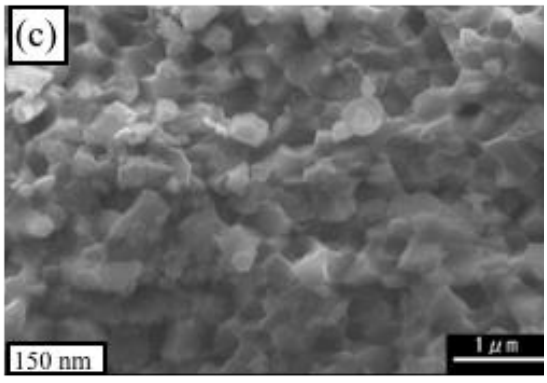


Fig. 6. SEM photographs for the fracture surfaces of $ZrO_2$(1.5Y)-25mol%$Al_2O_3$ ceramics sintered at: (a) 1573 K (1300°C), (b) 1598 K (1325°C), and (c) 1623 K (1350°C) for $6.0\times10^2$ s under 50 MPa. Average grain sizes are also shown at the bottom of each photograph.

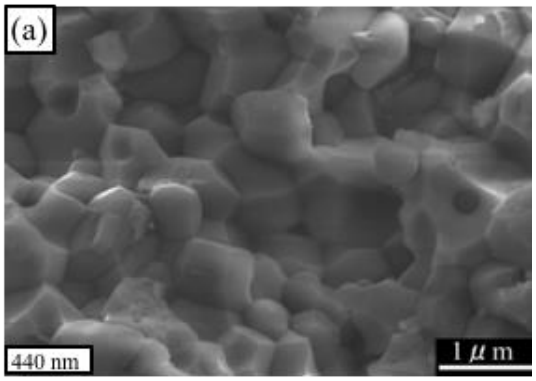


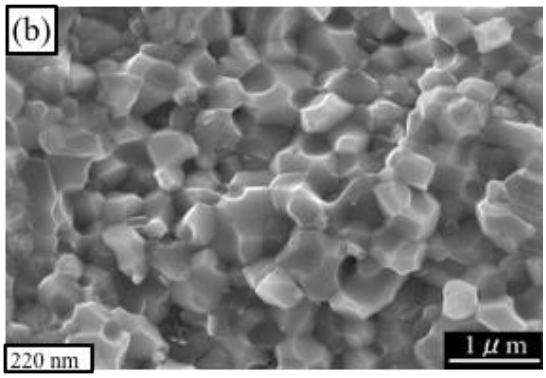


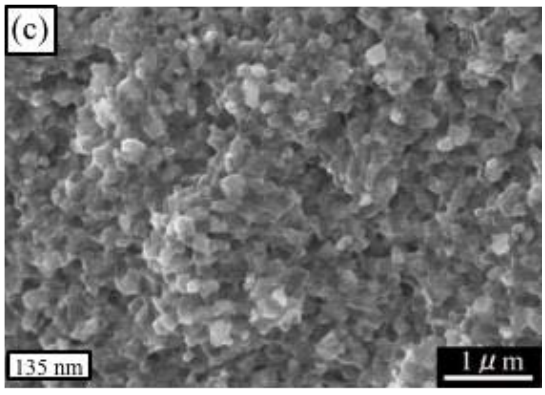


Fig. 7. SEM photographs for the fracture surfaces of the 1598 K (1325°C)-sintered $ZrO_2$($x$·mol%$Y_2O_3$)-25mol% $Al_2O_3$ ceramics; $x$= (a) 0.5, (b) 1.0, and (c) 2.0. Average grain sizes are also shown at the bottom of each photograph.

Figure 8 shows (1) the volume ratio (vol%) of $t$-$ZrO_2$ in $ZrO_2$ phase and (2) (a) the bulk ($D_{obs}$) and (b) relative ($D_{obs}/D_x$) densities as a function of $Y_2O_3$ content. This figure (1) reveals that the addition of more than 1.0 mol% $Y_2O_3$ increases the $t$-$ZrO_2$ vol% rapidly, and furthermore, as shown in (2), the addition of 1.5 mol% $Y_2O_3$ yielded the highest densities irrespective of the sintering temperature. It is very interesting that as little as 1.0 or 1.5 mol% $Y_2O_3$ was sufficient to stabilize $t$-$ZrO_2$ phase with high density. Conventional sintering methods, such as pressure less sintering, HP, or HIPping, require a slightly higher $Y_2O_3$ content *i.e.*, 2.0 or 3.0 mol% to attain the high $t$-$ZrO_2$ ratios and the high densities [2-10]. These differences between PECPS and conventional sintering might come from the high heating rate, *i.e.*, $1.67\times10^{-1}$ K·s$^{-1}$ (100 K·min$^{-1}$) and $8.33\times10^{-2}$ ~ $1.67\times10^{-1}$ K·s$^{-1}$ (5 ~ 10 K·min$^{-1}$) and short soaking time, $6.0\times10^{2}$ s (10 min) and $7.22\sim21.6\times10^{3}$ s (2~6 h), respectively. This rapid increasing temperature rate of PECPS could improve the sinter ability of powders by introducing a high electro-magnetic field effect. This effect has already been reported in studies employing the microwave or millimeter-wave sintering methods [28,29]. Furthermore, the short soaking time would suppress the grain growth during sintering.

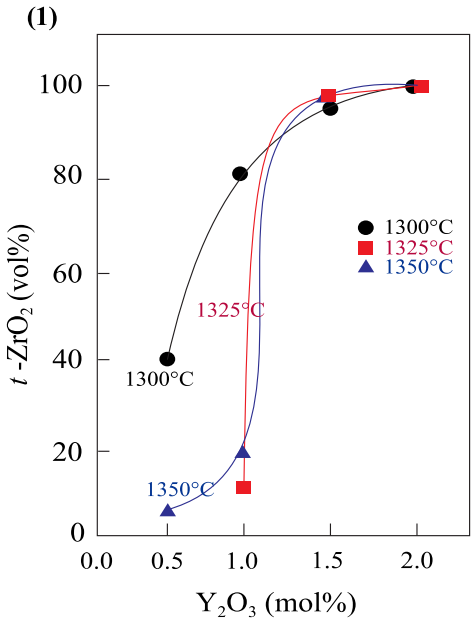


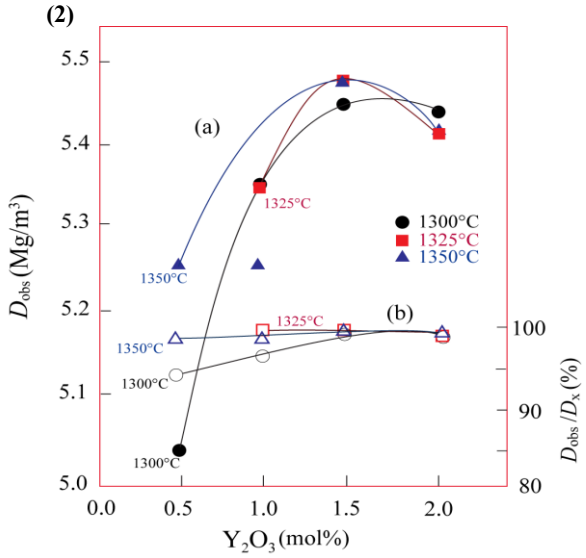


Fig. 8. (1) $t$-$ZrO_2$ volume ratio (vol%), (2) (a) bulk $D_{obs}$ and (b) relative $D_{obs}/D_x$ densities,

### 3.2 *Mechanical properties of ceramics*

The mechanical properties, such as a three-point bending strength ($\sigma_b$), fracture toughness ($K_{IC}$), and Vickers hardness ($H_v$), as a function of $Y_2O_3$ content are displayed in Fig. 9. Here, the values of $\sigma_b$ and $K_{IC}$, as already mentioned in the section of 2. Experimental procedure, Evaluation of samples, Mechanical properties**,** are evaluated using an 8mm-span and the IF method, respectively, to consider only the dependence of mechanical properties on the $Y_2O_3$ content and sintering temperature. It can be easily recognized that the addition of 1.5 mol% $Y_2O_3$ yielded the overall best data: $\sigma_b$ ≥1350 MPa, $K_{IC}$ ≥15.5 MPa·m$^{1/2}$, and $H_v$ ≥15.5 GPa in [1.5Y] ceramics sintered at 1598 K (1325°C). When we determined the $K_{IC}$ values using the Vickers IF method, we measured the average diagonal half length $a$ =76.3 μm, average crack half length $c$ =94.3 μm, therefore, $c/a$=1.23 < 2.5, and Palmqvist crack length $l$ =18.0 μm around the indent. To investigate the validity or effectivity of these best data, we fabricated large [1.5Y] ceramics (about 55 mm in diameter and 6.5 mm in thickness) from the same powder and process; their microstructural properties were bulk densities of 2.4 and

5.46 Mg·m$^{-3}$ powder and sintered compacts, respectively, relative density of ceramics more than 99.9%, *t*/*m*-$ZrO_2$ ratio of 88.7/11.3 vol%). Thus fabricated ceramics revealed a $\sigma_b$ of 1420 MPa determined using a 30mm-span, a $K_{IC}$ of 14.8 MPa·m$^{1/2}$, and a $H_v$ of 13.9 GPa [30]. From these values, the discrepancy between the small and large samples is not so high, or in other words, almost the same.

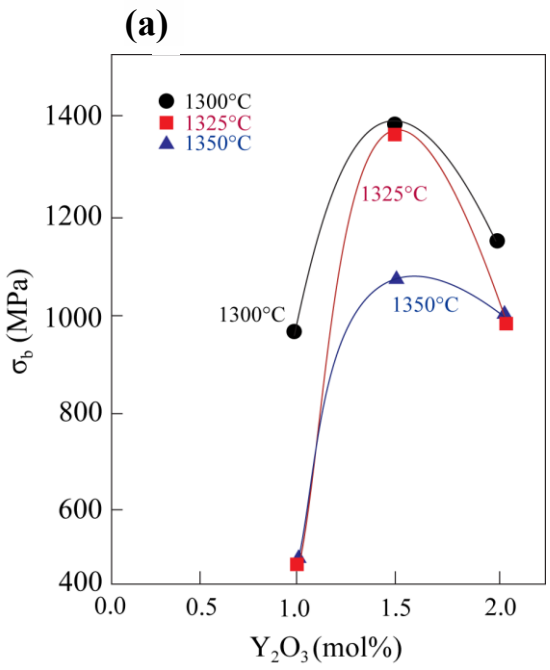


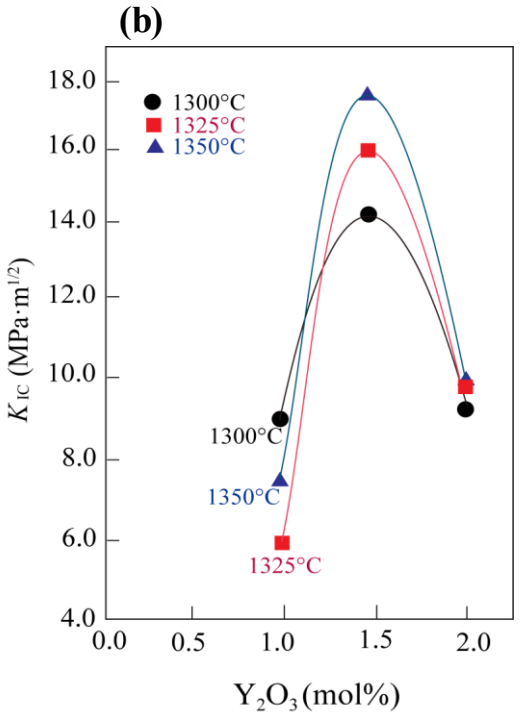


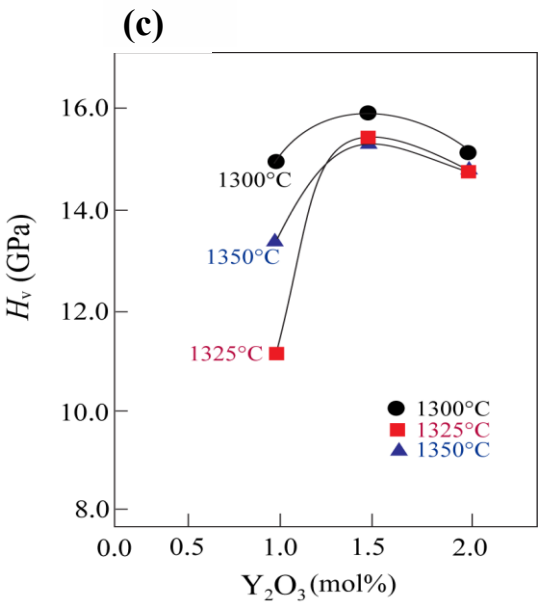


Fig. 9. (a) Three point bending strength $\sigma_b$, (b) fracture toughness $K_{IC}$, and (c) Vickers hardness $H_v$ of $ZrO_2$($x$·mol%$Y_2O_3$)-25mol%$Al_2O_3$ ceramics sintered at various temperatures as a function of $Y_2O_3$ content $x$.

The $K_{IC}$ values determined by the IF method has been investigated and compared with internationaly standardized fracture toughness test reported by Quinn *et al* [31]. They used the Standard Reference Material SRM2100 and showed the difference in $K_{IC}$ values among various IF technique (Niihara [14], Miyoshi [32], and Anstis [33]) as a function of indentation load; up to indentation load of 100 N, Niihara's eq. tends to give higher $K_{IC}$ values than those of SRM2100, however, Miyoshi's eq. seems to fortuitously match in once case, on the other hand, Anstis's eq. sometimes gives lower than those. However, when the indentation load increase to 196 N, their diremption also increase. Based on their data [31], as Niihara's $K_{IC}$ values are about 34% higher than those of SRM2100, Niihara's $K_{IC}$ values in the present best data (14.8 for the large to 15.5 for the small samples) should be reduced to 11.0 to 11.6 MPa·m$^{1/2}$.

Next, to investigate the origin of the high mechanical properties, the microstructures of the [1.5Y]

ceramics sintered at 1598 K (1325°C) were observed more precisely. Figure 10 shows: (a) a normal TEM bright field image; and (b) to (e) the elemental mappings for (b) Al, (c) O, (d) Zr and (e) Y on the same region. Comparison of these photographs reveals that the grey grains of $ZrO_2$ containing $Y_2O_3$ are surrounded homogeneously by white fine $\alpha$-$Al_2O_3$ particles segregated from the cubic $ZrO_2$ (*ss*) as mentioned before. This homogeneous distribution of $\alpha$-$Al_2O_3$ might be responsible for the high mechanical properties.

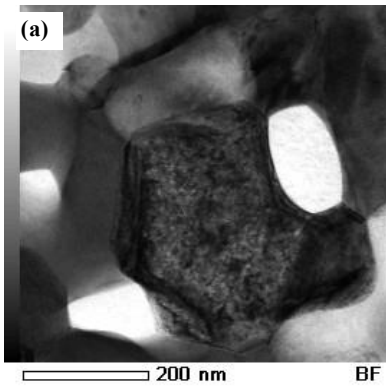


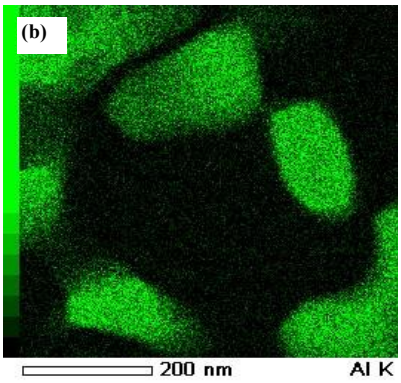


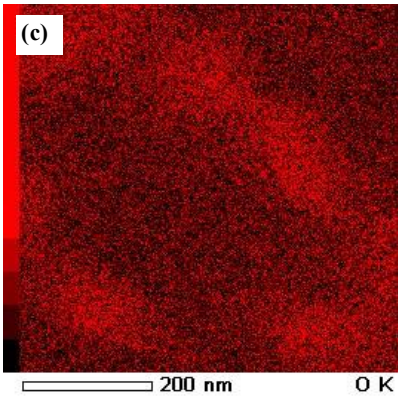


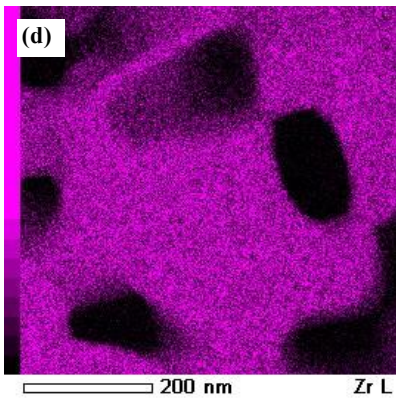


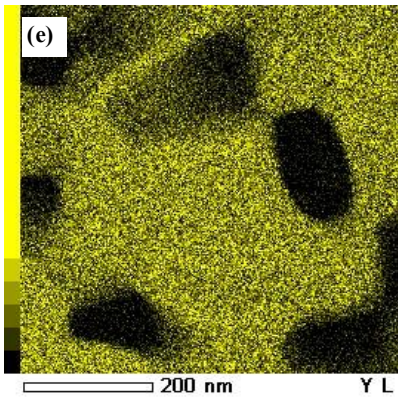


Fig. 10. TEM photographs of the microstructure for $ZrO_2$(1.5Y)-25mol%$Al_2O_3$ ceramics. (a) Bright field image and (b)~(e), elemental mapping of the same region: (b) Al, (c) O, (d) Zr and (e) Y.

To our knowledge the present study is the first report which describes the realization of both high $\sigma_b \geq 1$ GPa and high $K_{IC} \geq 11.0$ MPa·m$^{1/2}$ in the same ceramics. This can be explained by two mechanisms: i) the high $\sigma_b$ was achieved by a high relative density $\geq$ 99.9% with fine grain sizes around $\phi$140 nm, and ii) the high $K_{IC}$ occurred through the *t*- to *m*-$ZrO_2$ transformation toughening, which was induced by both a 25 mol% $Al_2O_3$ addition and a small amount of $Y_2O_3$ stabilizer. We should also note that a high $K_{IC}$ was attained by the homogeneous $Al_2O_3$ precipitates tightly surrounding the *t*-$ZrO_2$ grains; the former $Al_2O_3$ particles were decomposed from the *c*-$ZrO_2$(*ss*) powders prepared by the neutralization co-precipitation method. These are rather astonishing phenomena, because until now high

$\sigma_b$ and high $K_{IC}$ have not been attained simultaneously in the same sample; *i.e.*, they have always shown a trade-off relation. Therefore, these data are the first breakthrough ever in the history of engineering ceramics.

## 4. Conclusions

By utilizing both the *c*-$ZrO_2$(*ss*) powders corresponding to $ZrO_2$(1.5mol%$Y_2O_3$)-25mol%$Al_2O_3$ composition prepared by the neutralization co-precipitation method and the pulsed electric-current pressure sintering (PECPS), we fabricated dense $ZrO_2$-based composite ceramics consisting of fine *t*-$ZrO_2$ grains less than 150 nm surrounded by homogeneously dispersed $\alpha$-$Al_2O_3$ fine particles. These ceramics showed a high bending strength ≥1350 MPa and a high fracture toughness ≥15.5 MPa·$m^{1/2}$ (or ≥11.0 MPa·$m^{1/2}$) simultaneously, which has not been reported previously. This finding constitutes a new breakthrough in terms of a "trade-off relation" between $\sigma_b$ and $K_{IC}$ of engineering ceramics, which has previously been considered an intractable problem such as brittleness of ceramics due to the ionic or covalent bonding.

This work was supported by a grant to Research Centre for Advanced Science and Technology at Doshisha University and also financially supported by the Program for the Strategic Research Foundation at Private Universities, 2013-2017, the Ministry of Education, Culture, Sports, Science and Technology, Japan (project no. S1311036). The authors thank Ms. M. Toda and Ms. J. Morita of the Doshisha University Research Centre for Interfacial Phenomena for making the FE-SEM and FE-TEM observations of the samples.

## References

1) R.C. Garvie, R.H.J. Hannink, R.T. Pascoe, "Ceramic Steel?", *Nature*, **258** [5537], 703-704 (1975).
2) F.F. Lange, "Transformation Toughening-Part 3 Experimental Observations in the $ZrO_2$-$Y_2O_3$ System", *J. Mater. Sci.,* **17**, 240-246 (1982).
3) F.F. Lange, "Transformation Toughening-Part 4 Fabrication, Fracture Toughness and Strength of $Al_2O_3$-$ZrO_2$ Composites", *J. Mater. Sci.,* **17**, 247-254 (1982).
4) T.K. Gupta, F.F. Lange, J.H. Bechtold, "Effect of Stress-Induced Phase Transformation on the Properties of Polycrystalline Zirconia Containing Metastable Tetragonal Phase", *J. Mater. Sci.,* **13**, 1464-1470 (1978).
5) N. Claussen, "Stress Induced Transformation of Tetragonal $ZrO_2$ Particles in Ceramic Matrices", *J. Am. Ceram. Soc.,* **61**, 85-86 (1978).
6) R. Ruhle, N. Clausen, A.H. Heuer, Microstructural Studies of $Y_2O_3$-Containning Tetragonal $ZrO_2$ Polycrystal (Y-TZP), in N. Claussen, M. Ruhle, A. Heuer (eds.), *Science and Technology of Zirconia II*, *Advances in Ceramics*, **12**, (American Ceramic Society, Columbus, Ohio, 1984), pp.352-370.
7) K. Tsukuma, K. Ueda, K. Matsushita, M. Shimada, "High-Temperature Strength of $Y_2O_3$-Partially-Sabilized $ZrO_2$/$Al_2O_3$ Composites", *J. Am. Ceram. Soc.*, **68**, C-56- C-58 (1985).
8) T. Tsukuma, K. Ueda, M. Shimada, "Strength and Fracture Toughness of Isostatically Hot-Pressed Composites of $Al_2O_3$ and $Y_2O_3$-Partially-Stabilised $ZrO_2$", *J. Am. Ceram. Soc.*, **68**, C-4-C-5 (1985).
9) S. Hori, M. Yoshimura, S. Somiya, "Strength-Toughness Relations in Sintered and Isostatically Hot-Pressed $ZrO_2$-Toughened $Al_2O_3$", *J. Am. Ceram. Soc.*, **69**, 169-172 (1986).
10) T. Masaki, "Mechanical properties of toughened $ZrO_2$-$Y_2O_3$ ceramics", *J. Am. Ceram. Soc.*, **69**, 638-640 (1986).
11) A.M. Alper, Inter-Relationship of Phase Equilibria, Microstructure, and Properties in Fusion-Cast Ceramics, in G.H. Stewart(ed.), *Science of Ceramics*, **3**, **(**Academic Press, London, U.K., 1967), Fig. 2, p. 339.
12) S. Inamura, M. Miyamoto, Y. Imaida, M. Takagawa, K. Hirota, O. Yamaguchi, "High Fracture Toughness of $ZrO_2$ Solid-Solution Ceramics with Nanometre Grain Size in the System $ZrO_2$−$Al_2O_3$", *J. Mater. Sci. Let.,* **12**, 1368-1370 (1993)**.**
13) A.G. Evans, E.A. Charles, "Fracture Toughness Determination by Indentation", *J. Am. Ceram. Soc.*, **59**, 371-372 (1976).
14) K. Niihara, "A Fracture Mechanics Analysis of Indentation-Induced Palmqvist Cracks in Ceramics", *J. Mater. Sci. Lett.*, **2**, 221-223 (1983).

15) M. Tokita, “Trend in Advanced SPS Spark Plasma System and Technology”, *J. Soc. Powder Tech. Jpn.,* **30**, 790–804 (1993).

16) R. Orru, R. Licheri, A. M. Locci, A. Cinotti, G Cao, “Consolidation/Synthesis of Materials by Electric Current Activated/Assisted Sintering”, *Mater. Sci. Eng.*, **R. 63**, 127-287 (2009).

17) K. Hirota, K. Shibaya, H. Matsuda, M. Kato, H. Taguchi, “Fabrication of Novel $ZrO_2(Y_2O_3)$-$Al_2O_3$ Ceramics Having High Strength and Toughness Utilizing Pulsed-Electric Current Pressure Sintering (PECPS)”, *Advances in Applied Ceramics: Structural, Functional and Bioceramics*, **113**, 73-79 (2013).

18) K. Hirota, K. Shibaya, H. Matsuda, M. Kato, H. Taguchi, “Fabrication of Novel $ZrO_2(Y_2O_3)$-$Al_2O_3$ Ceramics Having High Strength and Toughness by Pulsed Electric-Current Pressure Sintering (PECPS) of Sol-Gel Derived Solid Solution Powders”, *The American Ceramic Society's Ceramic Transactions: Processing and Properties of Advanced Ceramics and Composites*, VI **249**, 3-13 (2014).

19) T. Tsukigata, K. Tsukuma, “Zirconia Powder-Raw Material for the Fabrication of High Strength and High Toughness Zirconia Ceramics”, *Ceramics,* **17**, 816-822 (1982).

20) Y. Ozaki, Ultrafine Zirconia Powder, in S. Somiya, M. Yoshimura (eds.) , *Zirconia Ceramics*, **1**, (Uchida Rokakuho, Tokyo, 2000), pp.31-44.

21) R.C. Garvie, P.S. Nicholson, “Phase Analysis in Zirconia Systems”, *J. Am. Ceram. Soc.*, **55,** 303-305 (1972).

22) Rietveld program ‘RIETAN’, http://fujioizumi.verse.jp/

23) M.I. Mendelson, “Average Grain Size in Polycrystalline Ceramics”, *J. Am. Ceram. Soc.*, **52**, 443–446 (1969).

24) S. Palmqvist, “Method att Bestamma Segheten hos Spread Materials”, *Sarkskilt Hardmetaller, Jernkortorets Ann.*, **141**, 300-7 (1957).

25) Y. Matsuno, H. Wakai, S. Sakaguchi, *Evaluation Technology Corpus of Mechanical Properties of Fine-Ceramics*, (Realize publisher, Tokyo, 1984), p.182.

26) K. Hirota, K. Yamamoto, K. Sasai, M. Kato, H. Taguchi, H. Kimura, M. Takai, M. Terada, “$Al_2O_3$-Compositional Dependence of Mechanical Properties of $ZrO_2$ Based Ceramics Fabricated from $ZrO_2(Y_2O_3)$-$Al_2O_3$ Solid Solution Powders”, *J. Jpn. Soc. Powder Powder Metall*., **60**[10], 428-435(2013).

27) R.P. Ingel, D. Lewis III, “Lattice Parameters and Density for $Y_2O_3$-Stabilized $ZrO_2$”, *J. Am. Ceram. Soc.,* **69**, 325-332 (1986).

28) H.D. Kimrey, J.O. Kiggans, M.A. Janney, R.L. Beatty, “Microwave Sintering of Zirconia-Toughened Alumina Composites”, *Mater. Res. Soc. Symp. Proc.,* **189**, 243-254 (1991).

29) M.A. Janney, H.D. Kimrey, “Microwave Sintering of Alumina at 28 GHz”, *Ceramic Powder Science*, **II**, 919-924, *Am. Ceram. Soc.*, (1988).

30) H. Kimura, K. Hirota, “Study on Mass-Production of Ceramics with High Strength and High Toughness Using $ZrO_2$-$Al_2O_3$ Solid Solution Powder”, *Final Report (on Release), AS2511267M, Japan Science and Technology Agency (JST),* (2014).

31) G.D. Quinn and R.C. Bradt, “On the Vickers Indentation Fracture Toughness Test”, *J. Am. Ceram. Soc.*, **90** [3] , 673-680 (2007).

32) T. Miyoshi, “A Study on Evaluation of $K_{IC}$ for Structural Ceramics”, *Trans. Jap. Soc. Mech. Eng. Ser. A.*, **51**A, 2489-97 (1985).

33) G.R. Anstis, P. Chantikul, B.R. Lawn, D.B. Marshal, “A Critical Evaluation of Indentation Techniques for Measuring Fracture Toughness: I, Direct Crack Measurements”, *J. Am. Ceram. Soc.*, **64** [9], 533-8 (1981).